Research reports

Circadian PER2::LUC rhythms in the olfactory bulb of freely moving mice depend on the SCN but not on behavior rhythms

Daisuke Ono[1], Sato Honma[2], and Ken-ichi Honma[2]

[1]Photonic Bioimaging Section, Research Center for Cooperative Projects, Hokkaido University Graduate School of Medicine, Sapporo, 060-8638, Japan
[2]Department of Chronomedicine, Hokkaido University Graduate School of Medicine, Sapporo, 060-8638, Japan

Corresponding authors: Sato Honma (sathonma@med.hokudai.ac.jp), and Ken-ichi Honma (kenhonma@med.hokudai.ac.jp)
Phone: +81-11-706-4737
Full address: North 15, West 7, Kita-ku, Sapporo, 060-8638, Japan

Running title
PER2::LUC rhythms in the OB of freely moving mice

Total number of page: 46
Total number of words in the whole manuscript: 7599, the abstract: 249, and the introduction: 477
Total number of figures: 6

Keywords: Behavior, Bioluminescence, Optical fiber, In vivo recording, VIP

Abstract

The temporal order of physiology and behavior in mammals is regulated by the coordination of the master circadian clock in suprachiasmatic nucleus (SCN) and peripheral clocks in various tissues outside the SCN. Because the circadian oscillator(s) in the olfactory bulb (OB) is regarded as SCN independent, we examined the relationship between the SCN master clock and circadian clock in OB. We also examined the role of vasoactive intestinal peptide receptor 2 (VPAC2) in the circadian organization of the OB. We continuously monitored the circadian rhythms of a clock gene product PER2 in the SCN and OB of freely moving mice by means of a bioluminescence reporter and an optical fiber implanted in the brain. Robust circadian rhythms were detected in the OB and SCN up to 19 days. Bilateral SCN lesions abolished the circadian behavior rhythms and disorganized the PER2 rhythms in the OB. The PER2 rhythms in the OB showed more than one oscillatory component of a similar circadian period, suggesting internal desynchronization of constituent oscillators. By contrast, significant circadian PER2 rhythms were detected in the VPAC2 deficient mice, despite the substantial deterioration or abolition of circadian

behavioral rhythms. These findings indicate that the circadian clock in the OB of freely moving mice depends on the SCN master clock but not on the circadian behavioral rhythms. The circadian PER2::LUC rhythm in the cultured OB was as robust as that in the cultured SCN but reset by slice preparation, suggesting that culturing of the slice reinforces the circadian rhythm.

Introduction

The temporal orders of physiology and behavior in mammals are regulated by the circadian system comprising the central pacemaker in the suprachiasmatic nucleus (SCN) and peripheral clocks in various tissues and organs. Structures in the brain outside the SCN also exhibit circadian oscillations in clock gene expression; however circadian rhythms in most of these structures damped in the absence of the SCN circadian pacemaker (Abe et al., 2002; Natsubori et al., 2013). Among aforementioned structure, the olfactory bulb (OB) appears to exhibit a unique circadian physiology. The OB shows strong signals of *Bmal1* (Honma et al., 1998), *Per1*, *Per2,* and *Clock* (Shieh, 2003) mRNA, particularly in the internal granular and mitral cell layer. The clock gene expression showed circadian rhythms (Namihira et al., 1999) which persist *ex vivo* with a period shorter than that shown in the SCN and are entrained by temperature cycle (Granados-Fuentes et al., 2004a). The OB also exhibits circadian rhythms in sensitivity to odors (Amir et al., 1999; Funk & Amir, 2000; Granados-Fuentes et al., 2006) and in olfaction (Miller et al., 2014). Multi-electrode recording of the dispersed OB neurons revealed that the circadian clock in the OB consisted of multiple

oscillators with different periods (Granados-Fuentes et al., 2004a). Direct connections from the SCN to the OB have not been identified, and the SCN signal is most likely indirectly transferred (Shipley & Adamek, 1984). Bilateral SCN lesions had no effect on the circadian *Per1-luc* rhythm in the cultured OB slice prepared 3 weeks after the lesions, suggesting that the SCN does not sustain the circadian rhythm in the OB (Granados-Fuentes et al., 2004b). These findings were confirmed by *in vivo* imaging in anesthetized rats (Abraham et al., 2005). On the other hand, the circadian rhythm of *Per2* expression in the OB was re-organized by a non-selective dopamine agonist, methamphetamine, in rats with bilateral SCN lesions (Natsubori et al., 2014). Thus, the OB is capable of independently oscillating in a circadian manner.

The neuropeptide vasoactive intestinal peptide (VIP) in the SCN is regarded as a mediator of intercellular coupling of circadian rhythms (Harmar et al., 2002; Aton et al., 2005; Maywood et al., 2005). VIP-containing neurons are also detected in the OB (Miller et al., 2014; Gracia-Llanes et al., 2003). Recently, Miller et al. (2014) reported that VIP deficient mice under isoflurane anesthesia failed to show the circadian

PER2::LUC rhythm in the OB in constant darkness (DD). However, this finding should be re-evaluated in conscious animals, because anesthesia was reported to alter circadian gene expression (Bellet et al., 2011; Cheeseman et al., 2012). In the present study, we developed an optical fiber recording system in freely moving mice which carried a bioluminescence reporter for a clock gene product PER2. We successfully demonstrate that the circadian rhythm in the OB depends on the SCN master clock but independent of the VIP signaling in the OB.

Materials and Methods

Animals

Male and female mice of C57BL/6j back ground were used at 3.5–7.0 months old. They carried a bioluminescence reporter of clock gene product PER2 (PER2::LUC mice) (Yoo et al., 2004). VIP receptor 2 (VPAC2) deficient (*Vipr2-/-*) mice of C57BL/6j back ground (Harmar et al., 2002) carrying a PER2::LUC reporter were also used. Mice were reared in our animal quarters where environmental conditions were controlled (lights-on, 6:00-18:00 h; light intensity, approximately 100 lx at the bottom of the cages;

humidity, 60 ± 10%). Mice had free access to food pellets and a water bottle. Experiments were conducted in compliance with the rules and regulations established by the Animal Care and Use Committee of Hokkaido University under the ethical permission of the Animal Research Committee of Hokkaido University (Approval No. 08-0279).

Behavioral activity measurement

Spontaneous movements were measured by a passive infrared sensor which detected a change in the intensity of thermal radiation from an animal due to movements (Abe et al., 2004). The amount of movement was recorded every one min by a computer software (The Chronobiology Kit: Stanford Software System, Santa Cruz, CA, USA).

Implantation of an optical fiber into the OB

Surgical operation was performed under isoflurane anesthesia. For the measurement of bioluminescence from the OB, a small hole in the skull was made using a dental drill bur (4.9 mm anterior to the bregma and 0.9 mm lateral from the mid line) and an optical fiber (1.5 mm depth from the skull surface) was stereotaxically inserted. The fiber was fixed to the skull with dental resin (Figure 1A).

More than 4 days after the insertion of the optical fiber, an osmotic pump containing luciferin, a substrate of luciferase, was implanted. To deliver the substrate to the OB, the osmotic pump (flow speed, 0.5 μl/h, pump volume; 200μl, 2002, Alzet, Cupertino, California, USA) was filled with D-luciferin K (100 mM) dissolved in physiological saline and implanted in the peritoneal cavity.

Implantation of an optical fiber into the SCN

To measure bioluminescence from the SCN, a handmade guide cannula (inner diameter 1.12 mm, outer diameter 1.48 mm) was stereotaxically inserted into the brain (0.2 mm posterior to the bregma and 0.2 mm lateral from the midline, and 3.0 mm from the surface of the skull) and fixed to the skull with dental resin. After a recovery period of more than 4 days, a polymethyl methacrylate optical fiber was inserted (fiber diameter, 0.5 mm; surface cladding, 0.25 mm thick) into the guide cannula aimed at the SCN (5.8 mm depth from the surface of the skull) and fixed to the skull with dental resin.

To deliver the substrate to the SCN, an L-shaped cannula (inner diameter 0.52 mm, outer diameter 0.80 mm) was stereotaxically inserted

into the lateral ventricle (0.6 mm posterior to the bregma, 1.4 mm lateral from the midline, and 2.2 mm from the surface of the skull). The cannula was connected through a catheter with an osmotic pump (flow speed, 0.11 μl/h; pump volume, 100μl, 1004, Alzet) filled with D-luciferin Na (50mM) in artificial cerebrospinal fluid and implanted subcutaneously in the midscapular area of the back. A catheter from the osmotic pump was passed under the skin to the L-shaped cannula. The implantation of an osmotic pump was performed more than 4 days after the insertion of the optical fiber.

Bilateral SCN lesions

Bilateral SCN lesions were performed stereotaxically in PER2::LUC mice under isoflurane anesthesia. Small holes were made in the skull using a dental drill bur (0.2 mm posterior to the bregma and 0.2 mm lateral from the mid line). A stainless steel electrode (0.3 mm in diameter; Unique Medical, Tokyo, Japan) coated entirely with epoxy resin except for the tip (0.3 mm in length), was inserted bilaterally into the SCN (5.8 mm depth from the surface of the skull). SCN lesion was generated by passing a direct electrical current of 3.0 mA for 12 s with an isolator (DPS-105, Nihon Denki Sanei, Tokyo, Japan). After the SCN lesions, spontaneous movements were

measured under LD for more than 16 days to confirm the loss of circadian rhythm. This measurement was done in a box where the light intensity was 300 lx in the light phase. Behaviorally arrhythmic mice were used for *in vivo* measurements. Subsequently, they were subjected to the implantation of an optical fiber in the OB and an osmotic pump in the peritoneal cavity as described in the preceding section. The measurement of bioluminescence started 20–42 days after the SCN lesions.

After each surgery, penicillin-G (Meiji Seika Pharma Co., Ltd., Tokyo, Japan) was used to prevent infection (40 unit/g of body weight, intra-muscular injection). We prescribed aspirin (120mg/kg of body weight, per os) for 3 days after surgery.

Histological examination

Once the measurements were completed, mice were anesthetized with ether and intracardially perfused with physiological saline, followed by 4% paraformaldehyde in 0.1M phosphate buffer (PB). Brains were cryoprotected with 20 % sucrose in 0.1M PB. Serial coronal sections of 30 μm thick were made using Cryostat (Leica, Biosystems, Nussloch, Germany) and stained with cresyl violet to identify the localization of the tip of the optical

fiber and to confirm the SCN lesions.

In vivo measurement of bioluminescence

Mice were individually housed in polycarbonate cages (115 mm wide, 215 mm long, and 300 mm high) placed in a light-tight and air-conditioned box (40 cm wide, 50 cm long, and 50 cm high; light intensity during the light phase, 150–250 lux LED light). Three to five days after the implantation of an osmotic pump, bioluminescence measured from the SCN or OB in freely moving mice under DD. The measurement was performed every one minute via an optical fiber. The fiber was at least 3 m long to ensure the animal's free movement and reduce fiber torque. The optical fiber was connected to a photon counting device (In vivo Kronos, Atto, Tokyo, Japan) equipped with a photo multiplier tube (Hamamatsu Photonics, Hamamatsu, Shizuoka, Japan). Recorded data were fed into a computer and analyzed.

Slice preparation and bioluminescence measurement in culture

Mice were euthanized by cervical dislocation and decapitated without anesthesia. Their brains were removed and coronal slices of 300 μm thick were made by a microslicer (DSK Microslicer™, Dosaka EM, Kyoto, Japan) in cooled Hanks' Balanced Salt solution (SIGMA). Trimmed bilateral SCN or

unilateral OB slices were placed on a culture membrane (Milicell-CM, Millipore Corporations, Billerica, Massachusetts, USA) in a 35-mm Petri dish. The slice was cultured in air at 36.5 °C with 1.2 ml Dulbecco's modified Eagle's medium (Invitrogen, Carlsbad, CA, USA) with 0.1 mM D-luciferin K and 5% supplement solution as described previously (Ono et al., 2013). Bioluminescence from the SCN or OB slices was measured for one min at 10-min intervals with a photon counting device (Lumicycle, Actimetrics, Wilmette, Illinoi, USA or Kronos, Atto, Tokyo, Japan). Bioluminescence intensity was expressed as relative light unit (RLU: counts/min).

Data analysis

Time series data of bioluminescence *in vivo* were smoothed by a four hour moving average method and detrended by a 24 h moving average subtraction method (Ono et al., 2013). A chi-square periodogram was used to evaluate of circadian rhythms with a significance level of $P < 0.01$. To compare the peak phases of circadian PER2::LUC rhythms between *in vivo* and *ex vivo* conditions, we used the midpoint of rising and falling limbs of the detrended circadian rhythm that intersected the X-axis.

The amplitude of the circadian rhythm was defined as the difference

between the maximum and minimum value of data in a cycle. The amplitude was standardized in such a way that each amplitude was divided by the peak level, because a strong positive correlation exists between the amplitude and peak level (Ono et al., 2013). The mean amplitude was calculated from the individual mean of standardized amplitudes measured during the first 10 days in DD. The maximum amplitude was defined as the largest amplitude during the first 10 days.

For the double plotting of bioluminescence data, the differences from the minimum value of the detrended data were used by ClockLab (Actimetrics). To compare group circadian rhythms, each value in individuals was normalized as a ratio of the 24 hour average in the first cycle of the measurement. A chi-square periodogram (with a significance level $P < 0.01$) was used for the detection of periodicity (ClockLab).

Sequential changes in the period and amplitude of circadian rhythm were characterized by wavelet analysis (Araszkiewicz & Bogusz, 2010). The continuous wavelet transform coefficient (CWTc) was calculated within a range of 12–36 h (Wavelet toolbox, MATLAB, Mathworks Inc., Natic, MA, USA). The bandwidth parameter was set to 3.0 and the center frequency to

1.0. Under these conditions, 3 cycles prior to and 3 cycles subsequent to a particular time contributed to CWTc at that point.

Statistics

A repeated measure two-way ANOVA with a post-hoc t test was applied to compare the two circadian profiles of group means. A repeated measure one-way ANOVA was applied to compare the circadian profiles of paired group means. Student's t-test was used to compare two independent group means. Welch's t-test was used when the variances of two group means were different. Paired t-test was used when two dependent group means were compared (Statview; SAS Statistics Inc., Cary, NC, USA, or Statcel 3; OMS Ltd., Saitama, Japan). Rayleigh test was used to examine the clustering of circadian phases in a circular analysis (Oriana4; RockWare, Inc., Golden, CO, United States).

Results

Circadian PER2::LUC rhythms in the OB of freely moving mice

Robust circadian PER2::LUC rhythms were detected in the OB of freely moving mice for 13 to 19 days under DD (Figures 1B-1E, Figure S1).

Chi-square periodogram revealed statistically significant circadian rhythms ($P < 0.01$) in PER2::LUC and behavioral activity (Figure 1F). The circadian rhythms in PER2::LUC were stable in both periodicity and amplitude as indicated by wavelet analysis (Figure 1G, Figure S1). *In vivo* circadian peak of PER2::LUC rhythm in the OB of mice kept under an LD cycle (lights-on 6:00-18:00 h) was observed in the middle of the subjective night on the first day of DD (22.6 ± 0.6 h in local time of the 1st cycle (LT_1), mean ± SD, n = 4). The trough of the circadian bioluminescent rhythm was located in the middle of the subjective day (10.9 ± 0.6 h LT_1) and bioluminescence started to increase before the circadian increase of behavioral activity (Figures 1B and 1C), indicating that the PER2::LUC rhythms were not a consequence of the circadian change in physical movement. The mean damping rate (a ratio of the decrement of amplitude in the 10th cycle to that on the 1st cycle) was 0.01 ± 0.07 (n = 4), indicating the remarkable stability of rhythmicity. The circadian periods of PER2::LUC and of behavioral rhythms were 23.9 ± 0.1 h and 23.9 ± 0.2 h, respectively and were not significantly different ($t_3 = -0.584$, $P = 0.700$, Paired t-test) (Figure 1F).

Resetting of circadian PER2::LUC rhythms in the OB but not in the SCN by slice preparation for culturing

To compare the circadian phase of PER2::LUC rhythm between *in vivo* and *ex vivo* conditions, we examined circadian rhythms of cultured OB slices (Figure 2). In this experiment, the effect of the time of day of decapitation and subsequent brain slice preparation on the circadian phase was systematically examined. The brains were sampled every 4 h and the OB and SCN were prepared for slice cultures. Circular analysis revealed that the 1st circadian peaks in the OB were scattered throughout the 24 h (P = 0.701, n = 12, Rayleigh test), while those in the SCN were significantly clustered (P = 1.08 × E-07, n = 12, Rayleigh test). By contrast, the circadian peaks in freely moving mice were significantly clustered in both the OB (22.6 ± 0.6 h LT_1, mean ± SD, P = 0.008, n = 4, Rayleigh test) and SCN (21.0 ± 0.1 h LT_1, P = 0.033, n = 3, Rayleigh test). The *in vivo* circadian peak of the SCN was calculated using the same animals as reported previously (Ono et al., 2015). In *ex vivo* experiment, the circadian peak in the SCN was detected at 17.9 ± 1.2 h LT_1 (n = 12), regardless of the time of brain sampling (Figure 2A and 2B). The *ex vivo* circadian peak was slightly but significantly phase

ahead of the *in vivo* peak ($t_{11.69}$ = 8.501, P = 2.01 × E-06, Welch's t-test). On the other hand, the circadian peak in the OB depended on the time of brain sampling (Figures 2A–2C). The peak was detected 25.3 ± 1.3 h (n = 12, mean ± SD) after decapitation. These *ex vivo* findings indicate that the circadian clock in the OB was reset by decapitation and/or following slice preparation. Such a resetting was not observed in SCN slices.

Bilateral SCN lesions internally desynchronize the circadian PER2::LUC rhythm in the OB of freely moving mice

Histological examination confirmed bilateral SCN lesions in all mice examined (Figure S2). Twenty to forty-two days after the SCN lesions, circadian behavioral rhythms were completely abolished but PER2::LUC rhythms in the OB persisted in freely moving mice (Figures 3A, 3B, Figure S3). Chi-square periodogram revealed more than one periodicity in the circadian range in PER2::LUC expression (Figure 3C, Figure S3). Four distinct periodicities were identified in most mice with SCN lesions. The mean and SD of each period for the first 10 days of recording was 20.7 ± 0.2 h (n = 4), 24.5 ± 0.9 h (n = 6), 28.3 ± 0.9 h (n = 5) and 31.6 ± 0.7 h (n = 5). By

closer inspection, the recurrence of circadian rhythms was detected at 3–5 cycle intervals with multiple non-circadian peaks in between. Wavelet analysis confirmed that the circadian periodicity waxed and waned in the course of measurement (Figure 3D, Figure S3).

Circadian PER2::LUC rhythms in the OB of Vipr2$^{-/-}$ mice in vivo and ex vivo

The circadian behavioral rhythms of *Vipr2*$^{-/-}$ mice were not robust or almost abolished (Figure 4, Figure S4). On the other hand, significant circadian PER2::LUC rhythms were observed in the OB of *Vipr2*$^{-/-}$ mice (Figure 4, Figure S4). In two mice (#1, #3), more than one periodicity in the circadian range was detected by Chi-square periodogram (Figure 4C, Figure S4). Wavelet analysis confirmed waxing and waning changes of the circadian rhythmicity (Figure 4D, Figure S4). The normalized 24 h profile of PER2::LUC on Day 1 was slightly but significantly different from wild type (WT) ($F_{1,23} = 1.763$, $P = 0.022$, two-way repeated measure ANOVA), showing a secondary small peak (Figure 4E).

The normalized circadian profile on Day 10 was the same as that on Day 1 in both WT and *Vipr2*$^{-/-}$ mice (Figures 4F and 4G). The maximum

amplitude of circadian rhythms in *Vipr2*$^{-/-}$ mice (0.166 ± 0.026, mean ± SD, t_6 = −0.374, P = 0.721, n = 4, Student's t-test) was almost the same as that in WT (Figures 1 and 4). The damping ratio in *Vipr2*$^{-/-}$ mice was 0.19 ± 0.07 (n = 4) and not significantly different from that in WT (t_6 = 1.564, P = 0.169, Student's t-test). The circadian peak of PER2::LUC rhythms in the OB of *Vipr2*$^{-/-}$ mice occurred at 18.9 ± 3.2 h LT_1 (n = 4). The circadian period in *Vipr2*$^{-/-}$ mice was 22.4 ± 1.5 h which was not significantly different from that in WT ($t_{3.01}$ = 2.050, P = 0.133, Welch's t-test).

Significant circadian PER2::LUC rhythms were also detected in the cultured OB slices of *Vipr2*$^{-/-}$ mice (Figures 5A and 5B). The standardized amplitudes of circadian rhythms on the 1st day of culture were not significantly different between *Vipr2*$^{-/-}$ and WT mice for both structures (SCN, WT: 0.41 ± 0.06, *Vipr2*$^{-/-}$: 0.33 ± 0.07, t_6 = 1.735, P = 0.133, Student's t-test; OB, WT: 0.43 ± 0.07, *Vipr2*$^{-/-}$: 0.53 ± 0.06, t_6 = −2.038, P = 0.087, Student's t-test), (Figure 5C). By contrast, the damping ratio was significantly larger in the *Vipr2*$^{-/-}$ mice than in WT for the SCN (WT: 0.12 ± 0.26, *Vipr2*$^{-/-}$: 0.52 ± 0.31, $F_{1,4}$ = 5.377, P = 0.003, two-way repeated measure ANOVA), but not for the OB (WT: 0.49 ± 0.40, *Vipr2*$^{-/-}$: 0.72 ± 0.19, $F_{1,4}$ =

0.430, $P = 0.785$, two-way repeated measure ANOVA) (Figure 5D).

Robustness and stability of in vivo circadian PER2::LUC rhythm

The *in vivo* circadian PER2::LUC rhythms in the OB of SCN lesioned mice were less strong and more variable than those in the OB of SCN intact mice (Figure 6). The mean max CWTc in individual mice remained lower in the SCN lesioned mice than that in the SCN intact controls (Figures 6A and 6D). The mean amplitude of PER2::LUC rhythms during the first 10 days under DD was also lower in the SCN lesioned mice than in the controls (Figure 6B). However the maximum amplitude of circadian PER2::LUC rhythm in the SCN lesioned mice was not significantly different from that in the controls during the course of measurement (Figure 6C), indicating a potential robustness of circadian rhythm at similar extent to the mice with intact SCN. On the other hand, the coefficient of variation (CV) of the mean max CWTc was significantly larger in the SCN lesioned mice than in the control (Figure 6E), indicating instability of the circadian rhythm.

The variability as well as the strength of circadian PER2::LUC rhythms in the OB of *Vipr2*$^{-/-}$ mice were not significantly different from those

in the WT control (Figure 6). Neither the mean nor the maximum amplitude of circadian rhythms was different between control and *Vipr2*$^{-/-}$ mice (Figures 6B and 6C). The same was the case for the mean max CWTc and CV of it (Figures 6D and 6E).

Discussion

Circadian PER2::LUC rhythm in the OB of freely moving mice

The circadian PER2::LUC rhythms in the OB of freely moving mice were robust and stable for up to 19 cycles under DD (Figure 1). They were in synchrony with circadian behavior rhythms but there was no evidence of causality between them. The circadian PER2::LUC rhythm started to elevate from the trough before the increase of behavioral activity (Figure 1B). In *Vipr2*$^{-/-}$ mice, the circadian PER2::LUC rhythms in the OB were well sustained, while the circadian behavioral rhythms were substantially disrupted (Figure 4). These discrepancies between the circadian PER2::LUC rhythms in the OB and behavioral rhythms indicate the independency of PER2::LUC rhythm in the OB from behavioral rhythm.

The SCN circadian pacemaker sustains the circadian system in the OB

Bilateral SCN lesions abolished the internal synchrony of the OB circadian system and caused several periodicities in the circadian range (Figure 3). The periods could be roughly categorized into 4 groups; 20 h, 24 h, 28 h, and 32 h. In the course of oscillation under DD, the robust circadian rhythm appeared only for 1 to 2 cycles, which was followed by splitting of the circadian rhythm into two or more components for several cycles. Robust circadian rhythms and split rhythms appeared alternatively, suggesting a beat phenomenon. The maximum amplitude of the circadian rhythm in the course of measurement was not significantly reduced by the SCN lesions, indicating that a transient circadian rhythm is comparable to the intact rhythm. Wavelet analysis demonstrated that circadian periodicity waxed and waned over the course of measurement, implying an alternating synchrony and desynchrony of more than one circadian oscillation with a slightly different period. Granados et al. (2004) demonstrated the circadian rhythm in firing rate of individual neurons in dispersed OB cell cultures. They found different circadian periods in different neurons in the same culture, ranging from 18.9 to 25.3 h. The findings suggest that the circadian

rhythm in the OB comprises multiple cellular rhythms coupled to each other.

In the OB, *Per2* is substantially expressed in the glomerular layer, the mitral cell layer and internal granular layer (Shieh, 2003). The functions of these layers are different and may possess respective circadian oscillators of different periods. Circadian rhythm in the number of c-Fos positive cells in the OB peaked at slightly different time of day in the mitral cell and granular cell layer (Granados-Fuentes et al., 2006), and the 24 h profile in the OB was different in the concentration of dopamine, an intrinsic neurotransmitter, and serotonin, a neurotransmitter of afferent projection (Corthell et al., 2013). The glomerular layer is the site of integration of odorant signals, the mitral cells are the principal output neurons of OB, and the granular cells are interneurons which convey afferent signals to the mitral cells (Mori, 2014).

Direct connections from the SCN to the OB have not been identified. But the OB seems to receive the circadian signals from the SCN indirectly, for example, through the locus coeruleus and raphe nucleus (Shipley & Adamek, 1984), from where noradrenergic and serotonergic fibers terminate in the granular and glomerular layer of the OB, respectively (McLean et al.,

1989; Gracia-Llanes et al., 2010). Monoamine concentrations in the OB including dopamine and serotonin were reported to vary with time of day (Corthell et al., 2013). Interestingly, a non-selective dopamine agonist, methamphetamine, desynchronized the OB circadian rhythms from the SCN circadian pacemaker in the SCN intact rats (Natsubori et al., 2013) and reorganized the OB circadian rhythms in rats with bilateral SCN lesions (Natsubori et al., 2014). Dopaminergic interneurons are located in the glomerular layer, where they participate in the processing of sensory inputs (Cave & Baker, 2009). The glomerular layer is the site of *Per1* and *Per2* mRNA expression (Shieh, 2003). Circadian signals from the SCN may reset the circadian oscillations in the OB through the granular cells and the dopaminergic system. However, output measures of the SCN pacemaker other than behavior activity such as body temperature and adrenal hormones are not excluded as a possible mediator of the SCN signal to the OB circadian system, because changes in these measures were reported to reset the circadian oscillations in peripheral tissues (Buhr et al., 2010; Balsalobre et al., 2000)

Previously, circadian rhythms in the rat OB were reported to persist

after the bilateral ablation of the SCN in both *ex vivo* (Granados-Fuentes et al., 2004b) and *in vivo* experiments (Abraham et al., 2005). These findings suggested that the OB contained a circadian oscillator(s) independent of and comparable to the master pacemaker in the SCN. In the present study, circadian PER2::LUC rhythms in the OB were substantially disorganized by the SCN lesions probably through desynchronization of constituent circadian oscillators. The discrepancy between the present findings and those of could be explained by the length of observation and the time resolution of circadian rhythm analysis. The results of previous study were based on a relatively short recording (two full circadian cycles) with a low time resolution (intermittent measurement at 4 h intervals), whereas in the present study the measurement continued up to 19 days at 1 min intervals. The alternating synchrony and desynchrony of the OB circadian system may have been missed in the previous study because of a short duration of measurement. The SCN circadian pacemaker is necessary for the circadian organization of PER2::LUC in the OB of freely moving mice.

The PER2::LUC rhythms in the OB of freely moving mice with SCN lesion were markedly different from those in cultured OB slices (Figure 2).

Robust circadian PER2::LUC rhythm persisted in cultured OB slices for at least 4 cycles in the absence of the SCN circadian pacemaker. A possible explanation for this difference between *in vivo* and *ex vivo* results is the time lag between the SCN lesions and measurement of circadian rhythms. The *in vivo* measurement was conducted several weeks after the SCN lesions, while the *ex vivo* measurement started immediately after separation from the SCN. The deterioration of circadian rhythmicity due to desynchronization of cellular circadian rhythms in the OB may take time. Another possible explanation is resetting of constituent circadian oscillations by brain preparation for culture. The circadian rhythm in the cultured OB is the resetting by slice preparation (Figure 2). The mechanism of resetting is unknown but probably related to ambient temperature, since the brain was cooled for slicing before culturing. Temperature is regarded as a universal resetting cue for the peripheral circadian oscillators (Buhr et al., 2010). By resetting, desynchronized circadian oscillations would synchronize to each other to show coherent circadian rhythms.

Circadian PER2::LUC rhythms in the OB of Vipr2$^{-/-}$ mice

VIP and its receptor VPAC2 are present in the OB of rats and mice (Millar et al., 2014; Dietl et al., 1980). Mice lacking VPAC2 (*Vipr2*$^{-/-}$) were reported to show deteriorated circadian behavioral rhythms and clock gene expression in the SCN under constant conditions (Harmar et al., 2002; Aton et al., 2005; Maywood et al., 2005). In the present study, we confirmed deterioration of circadian behavioral rhythm in *Vipr2*$^{-/-}$ mice.

Recently, Miller et al. (2014) described the importance of VIP for the circadian rhythms in PER2::LUC and odor detection in the mouse OB. Using *in vivo* imaging, they demonstrated the abolition of circadian PER2::LUC rhythm in the OB of VIP deficient mice kept in DD but not in LD, suggesting that VIP is a crucial for sustaining circadian oscillation in the absence of external timing cues. In the present study, we were able to demonstrate significant circadian PER2::LUC rhythms in the OB of freely moving *Vipr2*$^{-/-}$ mice in DD (Figure 4 and Figure S4) and in cultured OB slices obtained from *Vipr2*$^{-/-}$ mice (Figure 5). The damping rate as well as the 24 h profile of PER2::LUC in the OB were not significantly different between the *Vipr2*$^{-/-}$ and WT mice in both *in vivo* (Figure 4G) and *ex vivo* (Figure 5). These results indicate that VIP signaling in the OB is not necessary for the expression of

circadian PER2::LUC rhythm which is independent of the behavior rhythms. The discrepancy between our findings and those of the previous report may be due to the intermittent use of anesthesia in the previous study, which can modify circadian rhythms in gene expression (Bellet et al., 2011; Cheeseman et al., 2012).

Circadian PER2::LUC rhythms in ex vivo and in vivo

PER2::LUC in the cultured OB of *Vipr2*$^{-/-}$ mice (Figure 5) showed circadian rhythms comparable to those of WT mice, indicating that the circadian system in the OB is self-sustaining. Similar results were reported for other brain structures in *Vipr2*$^{-/-}$ mice (Hughes et al., 2011). However, most circadian rhythms in the brain structures outside the SCN eventually undergo dampening (Abe et al., 2002; Natsubori et al., 2014), suggesting that the internal synchrony is attenuated in *ex vivo*, probably because of a lack of reinforcement by internal time cues from the SCN and/or disruption of the structural organization by slicing. The *in vivo* circadian rhythms of some brain structures outside the SCN were reset by slice preparation (Figure 2, Guilding et al., 2009). It is unclear why circadian rhythms are reset in some

structures but not others. But resetting of the OB circadian rhythm by culturing may explain the apparent difference between *in vivo* and *ex vivo* observations pertaining to the robustness of the circadian PER2::LUC rhythm in absence of the SCN.

In the present study, despite of the substantial deterioration of circadian behavior rhythm in *Vipr2*$^{-/-}$ mice, *in vivo* circadian PER2::LUC rhythms in the OB were preserved without damping for at least 10 cycles in DD (Figure 4). The finding indicates that the circadian PER2::LUC rhythm in the OB is not a consequence of physical movements and suggests that the circadian system in the OB receives a regulation of the SCN master clock different from that for behavior rhythms.

In conclusion, the circadian PER2::LUC rhythm in the OB of freely moving mice is organized by the SCN circadian pacemaker, and independent of the circadian behavioral rhythm. The circadian system in the OB is sustained without the VIP system for at least 10 cycles in the absence of external time cue.

Acknowledgements

We thank J.S. Takahashi for supplying PER2::LUC mice, and M.H. Hastings for supplying *Vipr2*$^{-/-}$ mice. We also thank M. Shimogawara and H. Kubota for developing of the photon counting device, K. Baba for technical advice, M.P. Butler for intensive discussion, and Y. Yamaguchi and I. Tsuda for helpful advice on wavelet analysis. This work was supported in part by Creation of Innovation Centers for Advanced Interdisciplinary Research Areas Program, Ministry of Education, Culture, Sports, Science and Technology, Japan, The Uehara Memorial Foundation, Narishige Neuroscience Research Foundation, and JSPS KAKENHI (No. 24390055, 26860156).

Conflict of interest

The authors declare no competing financial interests.

Abbreviations

ANOVA, analysis of variance; CWTc, Continuous wavelet transform coefficient; CV, Coefficient of variation; DD, constant darkness; LD, light dark cycles; LT_1, local time of the 1st cycle; LUC, luciferase; OB, olfactory bulb; PMT, photo multiplier tube; RLU, relative light unit; SCN, suprachiasmatic nucleus; VIP, vasoactive intestinal peptide; *Vipr2-/-*, VPAC2 deficient; VPAC2, vasoactive intestinal peptide receptor 2; WT, wild type

Reference

Abe, H., Honma, S., Ohtsu, H. & Honma, K. (2004). Circadian rhythms in behavior and clock gene expressions in the brain of mice lacking histidine decarboxylase. *Brain Res. Mol. Brain Res.*, **124,** 178-187.

Abe, M., Herzog, E.D., Yamazaki, S., Straume, M., Tei, H., Sakaki, Y., Menaker, M. & Block, G.D. (2002). Circadian rhythms in isolated brain regions. *J. Neurosci.*, **22**, 350-356.

Abraham, U., Prior, J.L., Granados-Fuentes, D., Piwnica-Worms, D.R. & Herzog, E.D. (2005). Independent circadian oscillations of Period1 in specific brain areas in vivo and in vitro. *J. Neurosci.*, **25**, 8620-8626.

Amir, S., Cain, S., Sullivan, J., Robinson, B. & Stewart, J. (1999). In rats, odor-induced Fos in the olfactory pathways depends on the phase of the circadian clock. *Neurosci. Lett.,* **272**, 175-178.

Araszkiewicz, A. & Bogusz, J. (2010). Application of wavelet technique to the Earth tides observations analyses. *Marees Terrestres Bulletin d'Informations (BIM)*, **146**, 11789-11798.

Aton, S.J., Colwell, C.S., Harmar, A.J., Waschek, J. & Herzog, E.D. (2005). Vasoactive intestinal polypeptide mediates circadian rhythmicity and synchrony in mammalian clock neurons. *Nat. Neurosci.*, **8**, 476-483.

Balsalobre, A., Brown, S.A., Marcacci, L., Tronche, F., Kellendonk, C., Reichardt, H.M., Schütz, G. & Schibler, U. (2000). Resetting of circadian time in peripheral tissues by glucocorticoid signaling. *Science*, **289**, 2344-2347.

Bellet, M.M., Vawter, M.P., Bunney, B.G., Bunney, W.E. & Sassone-Corsi, P. (2011). Ketamine influences CLOCK:BMAL1 function leading to altered circadian gene expression. *PLoS One*, **6**, e23982.

Buhr, E.D., Yoo, S.H. & Takahashi, J.S. (2010). Temperature as a universal resetting cue for mammalian circadian oscillators. *Science*, **330**, 379-385.

Cave, J.W. & Baker, H. (2009). Dopamine systems in the forebrain. *Adv Exp. Med. Biol.*, **651**, 15-35.

Cheeseman, J.F., Winnebeck, E.C., Millar, C.D., Kirkland, L.S., Sleigh, J., Goodwin, M., Pawley, M.D., Bloch, G., Lehmann, K., Menzel, R. & Warman, G.R. (2012). General anesthesia alters time perception by

phase shifting the circadian clock. *Proc. Natl. Acad. Sci. U. S. A.*, **109**, 7061-7066.

Corthell, J.T., Stathopoulos, A.M., Watson, C.C., Bertram, R. & Trombley, P.Q. (2013). Olfactory bulb monoamine concentrations vary with time of day. *Neuroscience*, **247**, 234-241.

Dietl, M.M., Hof, P.R., Martin, J.L., Magistretti, P.J. & Palacios, J.M. (1980). Autoradiographic analysis of the distribution of vasoactive intestinal peptide binding sites in the vertebrate central nervous system: a phylogenetic study. *Brain Res.*, **520**, 14-26.

Funk, D. & Amir, S. (2000). Circadian modulation of fos responses to odor of the red fox, a rodent predator, in the rat olfactory system. *Brain Res.*, **866**, 262-267.

Gracia-Llanes, F.J., Crespo, C., Blasco-Ibáñez, J.M., Marqués-Marí, A.I. & Martínez-Guijarro, F.J. (2003). VIP-containing deep short-axon cells of the olfactory bulb innervate interneurons different from granule cells. *Eur. J. Neurosci.*, **18**, 1751-1763.

Gracia-Llanes, F.J., Blasco-Ibáñez, J.M., Nácher, J., Varea, E., Liberia, T., Martínez, P., Martínez-Guijarro, F.J. & Crespo, C. (2010). Synaptic connectivity of serotonergic axons in the olfactory glomeruli of the rat olfactory bulb. *Neuroscience* **169**, 770-780.

Granados-Fuentes, D., Saxena, M.T., Prolo, L.M., Aton, S.J. & Herzog, E.D. (2004a). Olfactory bulb neurons express functional, entrainable circadian rhythms. *Eur. J. Neurosci.*, **19**, 898-906.

Granados-Fuentes, D., Prolo, L.M., Abraham, U. & Herzog, E.D. (2004b). The suprachiasmatic nucleus entrains, but does not sustain, circadian rhythmicity in the olfactory bulb. *J. Neurosci.*, **24**, 615-619.

Granados-Fuentes, D., Tseng, A. & Herzog, E.D. (2006). A circadian clock in the olfactory bulb controls olfactory responsivity. *J. Neurosci.*, **26**, 12219-12225.

Guilding, C., Hughes, A.T., Brown, T.M., Namvar, S., & Piggins, H.D. (2009) A riot of rhythms: neuronal and glial circadian oscillators in the mediobasal hypothalamus. *Mol. Brain.*, **2**, 10.1186/1756-6606-2-28.

Harmar, A.J., Marston, H.M., Shen, S., Spratt, C., West, K.M., Sheward, W.J., Morrison, C.F., Dorin, J.R., Piggins, H.D., Reubi, J.C., Kelly, J.S., Maywood, E.S., & Hastings, M.H. (2002). The VPAC(2) receptor is essential for circadian function in the mouse suprachiasmatic nuclei. *Cell*, **109**, 497-508.

Honma, S., Ikeda, M., Abe, H., Tanahashi, Y., Namihira, M., Honma, K. & Nomura, M. (1998). Circadian oscillation of BMAL1, a partner of a mammalian clock gene Clock, in rat suprachiasmatic nucleus. *Biochem. Biophys. Res. Commun.*, **250**, 83-87.

Hughes, A.T., Guilding, C. & Piggins, H.D. (2011). Neuropeptide signaling differentially affects phase maintenance and rhythm generation in SCN and extra-SCN circadian oscillators. *PloS One*, **6**, 10.1371/journal.pone.0018926.

Maywood, E.S., Reddy A.B., Wong, G.K., O'Neill, J.S., O'Brien, J.A., McMahon, D.G., Harmar, A.J., Okamura, H. & Hastings, M.H. (2006). Synchronization and maintenance of timekeeping in suprachiasmatic circadian clock cells by neuropeptidergic signaling. *Curr. Biol.*, **16**, 599-605.

McLean, J.H., Shipley, M.T., Nickell, W.T., Aston-Jones, G. & Reyher, C.K. (1989). Chemoanatomical organization of the noradrenergic input from locus coeruleus to the olfactory bulb of the adult rat. *J. Comp. Neurol.*, **285**, 339-349.

Miller, J.E., Granados-Fuentes, D., Wang, T., Marpegan, L., Holy, T.E. & Herzog, E.D. (2014). Vasoactive intestinal polypeptide mediates circadian rhythms in mammalian olfactory bulb and olfaction. *J. Neurosci.*, **34**, 6040-6046.

Mori, K. (eds), (2014). The Olfactory System. From Odor Molecules to Motivational behaviors. Springer, Tokyo, pp 1-206.

Namihira, M., Honma, S., Abe, H., Tanahashi, Y., Ikeda, M. & Honma, K. (1999). Daily variation and light responsiveness of mammalian clock gene, Clock and BMAL1, transcripts in the pineal body and different areas of brain in rats. *Neurosci. Lett.*, **267**, 69-72.

Natsubori, A., Honma, K. & Honma, S. (2013). Differential responses of circadian Per2 rhythms in cultured slices of discrete brain areas from rats showing internal desynchronisation by methamphetamine. *Eur. J. Neurosci.*, **38**, 2566-2571.

Natsubori, A., Honma, K. & Honma, S. (2014). Dual regulation of clock gene Per2 expression in discrete brain areas by the circadian pacemaker and methamphetamine-induced oscillator in rats. *Eur. J. Neurosci.*, **39**, 229-240.

Ono, D., Honma, S. & Honma, K. (2013). Cryptochromes are critical for the development of coherent circadian rhythms in the mouse suprachiasmatic nucleus. *Nat. Commun.*, **4**, 10.1038/ncomms2670.

Ono, D., Honma, K. & Honma, S. (2015). Circadian and ultradian rhythms of clock gene expression in the suprachiasmatic nucleus of freely moving mice. *Sci. Rep.* **5**, 10.1038/srep12310.

Shieh, K.R. (2003). Distribution of the rhythm-related genes rPERIOD1, rPERIOD2, and rCLOCK, in the rat brain. *Neuroscience*, **118**, 831-843.

Shipley, M.T. & Adamek, G.D. (1984). The connections of the mouse olfactory bulb: a study using orthograde and retrograde transport of wheat germ agglutinin conjugated to horseradish peroxidase. *Brain Res. Bull.*, **12**, 669-688.

Yoo, S.H., Ko, C.H., Lowrey, P.L., Buhr, E.D., Song, E.J., Chang, S., Yoo, O.J., Yamazaki, S., Lee, C. & Takahashi, J.S. (2004). PERIOD2::LUCIFERASE real-time reporting of circadian dynamics reveals persistent circadian oscillations in mouse peripheral tissues. *Proc. Natl. Acad. Sci. U. S. A.*, **101**, 5339-5346.

Figure legends

Figure1: Circadian PER2::LUC rhythms in the OB in freely moving mice

(A) Illustrations of a mouse implanted with an optical fiber (black line) and an overhead view of a hole for fiber implantation (left and middle). A red circle shows the area to which an optical fiber was inserted. Photograph of coronal section of the OB stained with cresyl violet demonstrates an optical fiber inserted into the granule cell layer (right). Small letters (d, v, m, and l) indicate the dorsal, ventral, medial, and lateral sides of the OB, respectively. A scale bar: 1.0 mm. (B) A representative PER2::LUC rhythm (red line) in the OB on the 1st day in DD with simultaneously measured spontaneous movements (black histogram). PER2::LUC bioluminescence is expressed in relative light unit (RLU). (C) Normalized group data of PER2::LUC rhythm and spontaneous movements on the 1st day in DD. Red line and pink area indicate the mean and SD of PER2::LUC rhythm, respectively. (D) A representative circadian bioluminescent rhythm (red) is illustrated in a sequential manner together with behavioral rhythm (black) measured simultaneously. Vertical solid lines indicate the local time 6:00 h. (E) A

double-plotted PER2::LUC rhythm in the OB (upper, red) and of behavioral rhythm (lower, black). (F) Results of Chi-square periodogram for PER2::LUC rhythm (upper) and behavioral rhythm (lower). The ordinate in the periodogram indicates Qp. The abscissa indicates the period of rhythmicity. The level of significance (oblique line in the panel) is set at $P < 0.01$. (G) Wavelet analysis of circadian rhythms in bioluminescence and behavioral activity. Levels of CWTc are expressed as a heatmap. At each time point, the highest CWTc in the range of 12–36 h is designated as the max CWTc. CWTc greater than the mean + 3SD of the max CWTc are shown in red. The mean max CWTc was calculated by excluding the first and last 3 days.

Figure2: Resetting of circadian PER2::LUC rhythms in the OB but not in the SCN by slice preparation for culturing

(A) Circadian PER2::LUC rhythms in the cultured SCN (n = 12) and OB (n = 12) for the first 3 days. Different colors indicate slices prepared at different times of day. The slices were prepared at 4-h intervals. Horizontal gray and black bars on the bottom of each panel indicate the light and dark phases of the LD cycle on the day of brain preparation. Vertical solid lines in each

panel indicate the local time of 6:00 am. Bioluminescence values are standardized in reference to the 1st circadian peak level defined as 1 and the subsequent trough level as 0 in individual slices. (B) Distribution of circadian PER2::LUC peaks on the 1st culture day in the SCN and OB plotted in a Rayleigh circle. Closed squares of different colors on the circumference indicate the peak phases of individual circadian rhythms (black: *in vivo*; colors: *ex vivo*). Arrow heads indicate the mean peak phases (black: *in vivo*; red: *ex vivo*) and the length of the arrow represents the extent of clustering of peak phases. Peak phases were significantly clustered in the SCN and OB *in vivo* (SCN: $P = 0.033$; OB: $P = 0.008$). In the OB *ex vivo*, clustering was not significant ($P = 0.701$). (C) Circadian peak phases of PER2::LUC rhythms in the OB slices are illustrated for 5 cycles in culture. The brain slices (n = 12) obtained at different circadian phases are indicated by different colors. The ordinate indicates the times of slice preparation. Two different slices were examined for each time.

Figure3: PER2::LUC rhythms in the OB of SCN lesioned mice

(A) A representative circadian bioluminescent rhythm (red) of an SCN

lesioned mouse is illustrated in a sequential manner together with simultaneously measured behavior activity (black). Vertical solid lines indicate the local time of 6:00 am. (B) Double-plotted PER2::LUC rhythm (upper, red) and behavior rhythm (lower, black) of the animal shown in (A). (C) Chi-square periodogram of PER2::LUC and behavioral rhythms in the animal shown in (B). See also Figure 1F. (D) Wavelet analysis of circadian rhythms in bioluminescence and behavioral activity. CWTc is expressed as a heatmap. See also the Figure 1G.

Figure4: PER2::LUC rhythms in the OB of *Vipr2*$^{-/-}$ mice

(A) A representative circadian bioluminescent rhythm (red) and simultaneously measured behavior rhythm (black) in a *Vipr2*$^{-/-}$ mouse are illustrated in a sequential manner. Vertical solid lines indicate the local time of 6:00 am. (B) Double plotted PER2::LUC rhythm (upper, red) and behavior rhythm (lower, black) of the animal shown in (A). See also Figure 1E. (C) Results of Chi-square periodogram of PER2::LUC rhythm and behavioral rhythm in the same mouse as (B). See also Figure 1F. (D) Wavelet analysis of circadian rhythms in bioluminescence and behavioral activity. CWTc is

expressed as a heatmap. See also the Figure 1G. (E) The mean 24-h profiles of PER2::LUC in the OB of wild type (WT) (open circle) and *Vipr2*$^{-/-}$ (closed circle) mice on day 1. The profiles are also compared between Day 1 and 10 in the WT (F) and *Vipr2*$^{-/-}$ (G) mice. Values are expressed as the mean and SD (WT, n = 4; *Vipr2*$^{-/-}$, n = 4). Two-way repeated measure ANOVA revealed significant difference between the WT and *Vipr2*$^{-/-}$ mice on Day1 ($F_{1,23} = 1.763$, $P = 0.022$). *, $P < 0.05$, vs. WT (post-hoc t-test). No significant difference was detected between Day 1 and 10 in either group.

Figure 5: Circadian rhythms of PER2::LUC in the cultured OB slice of *Vipr2*$^{-/-}$ mice

(A) Representative circadian rhythms of PER2::LUC in the cultured OB slices of the WT (upper) and *Vipr2*$^{-/-}$ (lower) mice. The circadian rhythms are detrended. (B) Chi-square periodograms reveal a significant circadian periodicity ($P < 0.01$). (C) Normalized amplitudes on Day 1 of culture and (D) damping rates were not different between the WT and *Vipr2*$^{-/-}$ mice.

Figure 6: Wavelet analysis of circadian PER2::LUC rhythms in the OB

(A) Max CWTc for PER2::LUC rhythm in the circadian range. Max CWTc are demonstrated in the course of measurement from Days 1 to 11 in the OB of control (SCN intact, upper), *Vipr2*$^{-/-}$ (middle) and SCN lesioned mice (lower). Colored lines in each panel indicate the max CWTc of different mice. The max CWTc in the first 3 days is biased because of a lack of sufficient data. (B) The mean amplitude of circadian PER2::LUC rhythm in the OB of control (SCN-intact), *Vipr2*$^{-/-}$ and SCN lesioned mice. The values are expressed as the mean and SD. Asterisks indicate statistically significant differences (*, $P < 0.05$, control or *Vipr2*$^{-/-}$ vs. SCN lesioned mice, one-way ANOVA with a post-hoc Tukey-Kramer test). (C) Maximum amplitude of circadian PER2::LUC rhythm in the OB of the control, *Vipr2*$^{-/-}$ and SCN lesioned mice. The values are expressed as the mean and SD. (D) Mean max CWTc of each group and SD. Results of the first three days are not included in the calculation. The mean max CWTc was significantly different among three conditions ($F_{2,11} = 10.317$, $P = 0.002$, one-way ANOVA), indicating a different strength of circadian periodicity. Asterisks indicate statistically significant differences (**, $P < 0.01$, control vs. SCN lesioned mice; *, $P < 0.05$, *Vipr2*$^{-/-}$ vs. SCN lesion, one-way ANOVA with a post-hoc Tukey-Kramer test). (E)

Variability of max CWTc for each condition. Variability is expressed as CV of the mean max CWTc in individual mice. CV (SD/mean) was significantly different among three conditions ($F_{2,11} = 7.537$, $P = 0.009$, one-way ANOVA). An asterisk (*) indicates statistically significant difference ($P < 0.05$, control vs. SCN lesion, one-way ANOVA with a post-hoc Tukey-Kramer test).

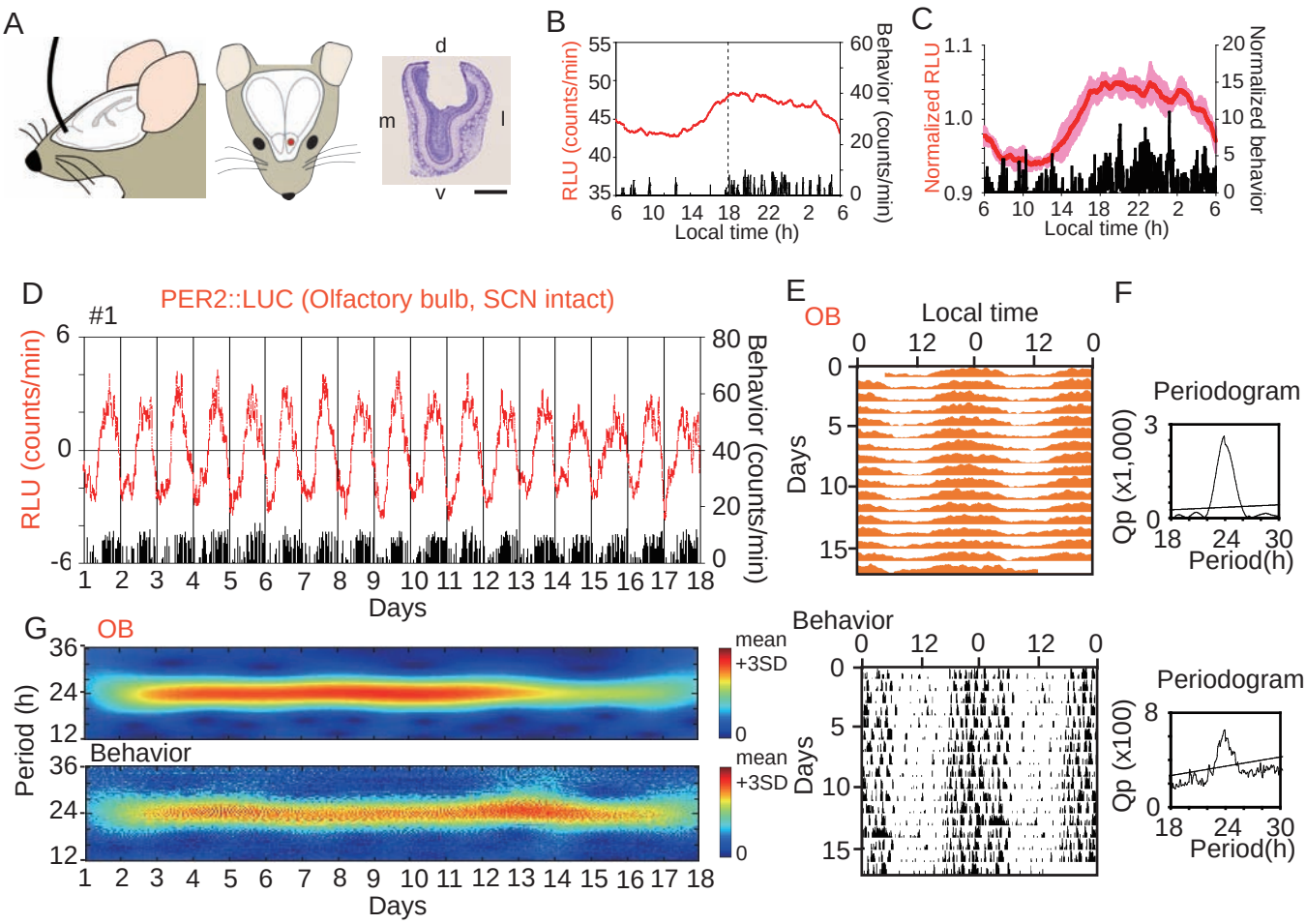
A
d
m
l
v
B
RLU (counts/min)
Behavior (counts/min)
Local time (h)
C
Normalized RLU
Normalized behavior
Local time (h)
D
PER2::LUC (Olfactory bulb, SCN intact)
#1
RLU (counts/min)
Behavior (counts/min)
Days
E
OB
Local time
Days
F
Periodogram
Qp (x1,000)
Period(h)
G
OB
Period (h)
mean
+3SD
Behavior
Days
Behavior
Periodogram
Qp (x100)
Period(h)

Figure 1

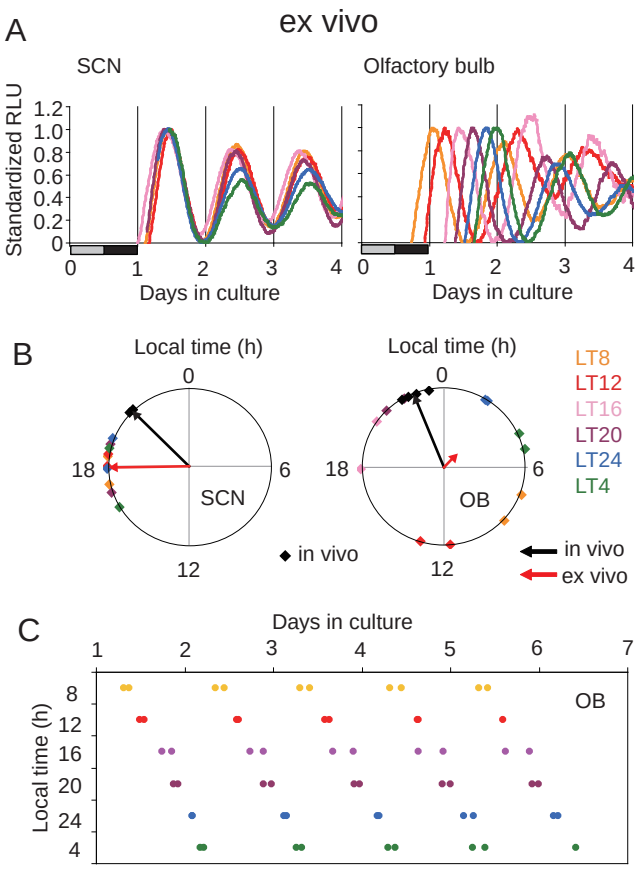
A
ex vivo
SCN
Olfactory bulb
Standardized RLU
1.2
1.0
0.8
0.6
0.4
0.2
0
0 1 2 3 4
Days in culture
0 1 2 3 4
Days in culture
B
Local time (h)
0
18
6
12
SCN
in vivo
Local time (h)
0
18
6
12
OB
LT8
LT12
LT16
LT20
LT24
LT4
in vivo
ex vivo
C
Days in culture
1 2 3 4 5 6 7
Local time (h)
8
12
16
20
24
4
OB

Figure 2

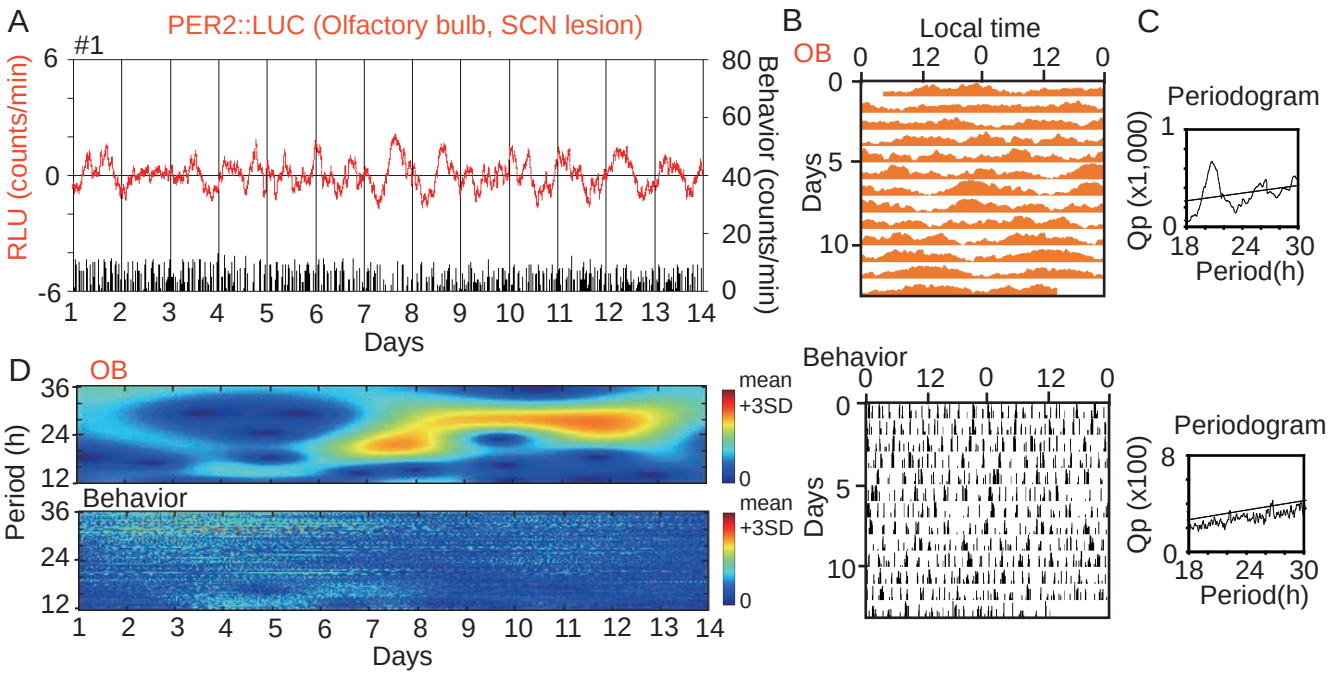
A
PER2::LUC (Olfactory bulb, SCN lesion)
#1
RLU (counts/min)
Behavior (counts/min)
Days
B
Local time
OB
Days
C
Periodogram
Qp (x1,000)
Period(h)
D
OB
Period (h)
mean
+3SD
Behavior
Behavior
Days
Periodogram
Qp (x100)
Period(h)

Figure 3

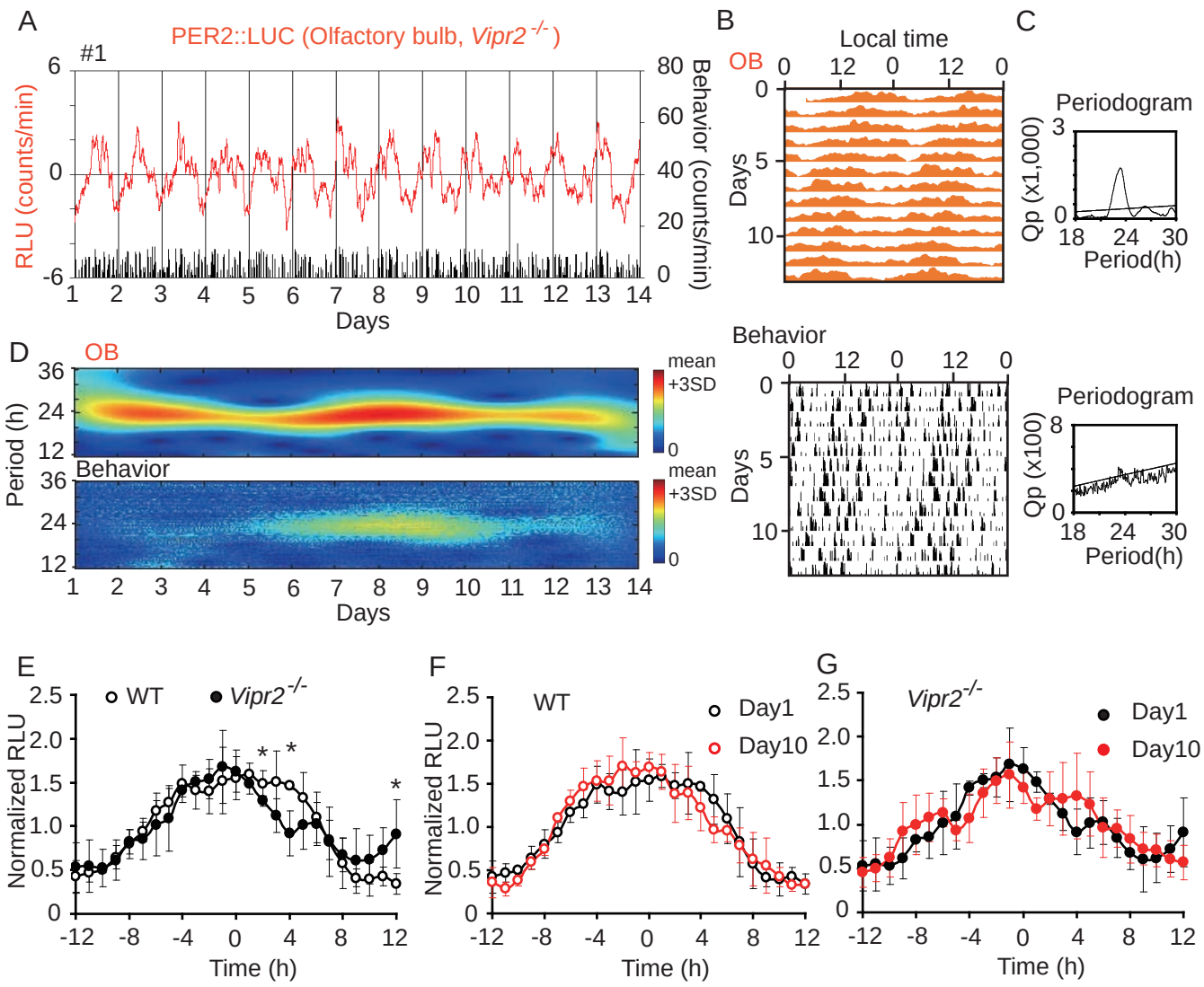
A
PER2::LUC (Olfactory bulb, Vipr2 -/-)
#1
RLU (counts/min)
Behavior (counts/min)
Days
B
Local time
OB
Days
C
Periodogram
Qp (x1,000)
Period(h)
D
OB
Period (h)
mean
+3SD
Behavior
Days
Behavior
Periodogram
Qp (x100)
Period(h)
E
WT
Vipr2 -/-
Normalized RLU
Time (h)
F
WT
Day1
Day10
Normalized RLU
Time (h)
G
Vipr2 -/-
Day1
Day10
Time (h)

Figure 4

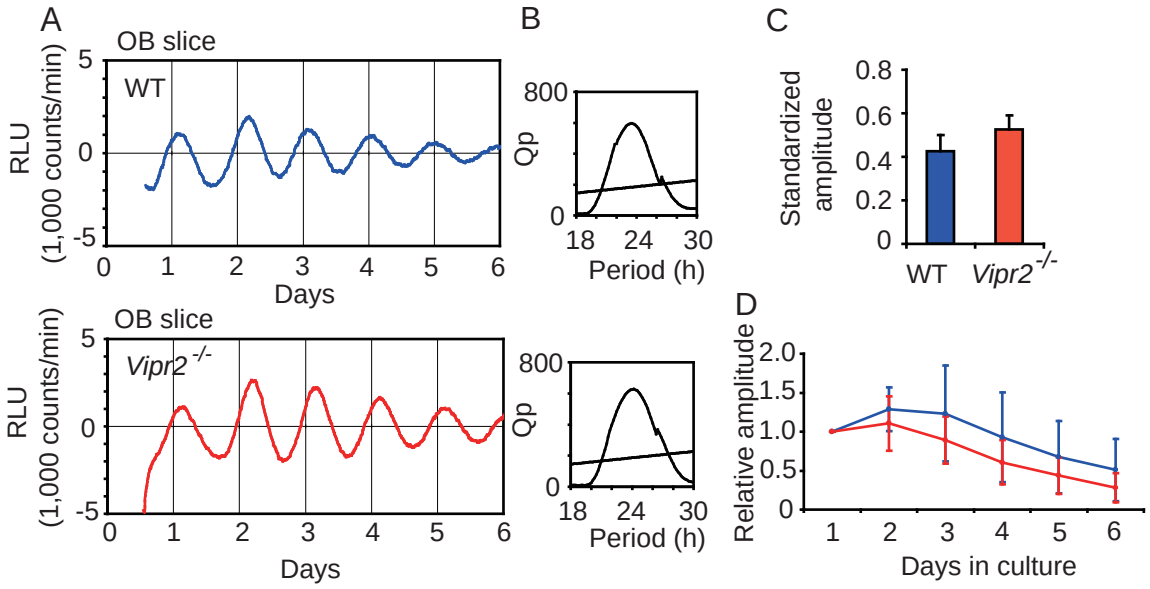
A
OB slice
WT
RLU
(1,000 counts/min)
5
0
-5
0 1 2 3 4 5 6
Days
B
800
Qp
0
18 24 30
Period (h)
C
Standardized amplitude
0.8
0.6
0.4
0.2
0
WT
Vipr2-/-
OB slice
Vipr2 -/-
RLU
(1,000 counts/min)
5
0
-5
0 1 2 3 4 5 6
Days
800
Qp
0
18 24 30
Period (h)
D
Relative amplitude
2.0
1.5
1.0
0.5
0
1 2 3 4 5 6
Days in culture

Figure 5

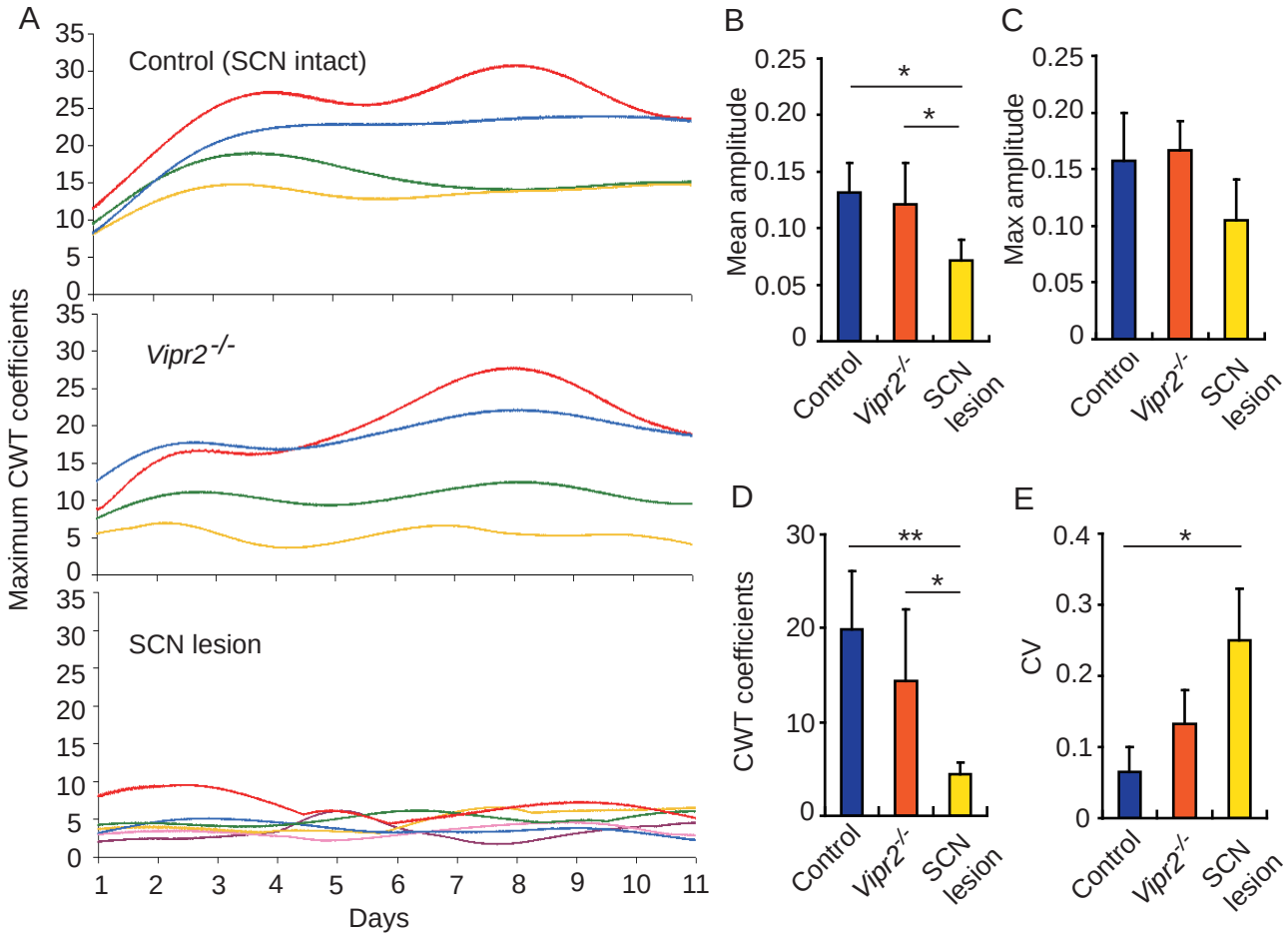
A
Control (SCN intact)
Vipr2-/-
SCN lesion
Maximum CWT coefficients
Days
B
Mean amplitude
C
Max amplitude
D
CWT coefficients
E
CV
Control
Vipr2-/-
SCN lesion

Figure 6

SCN intact

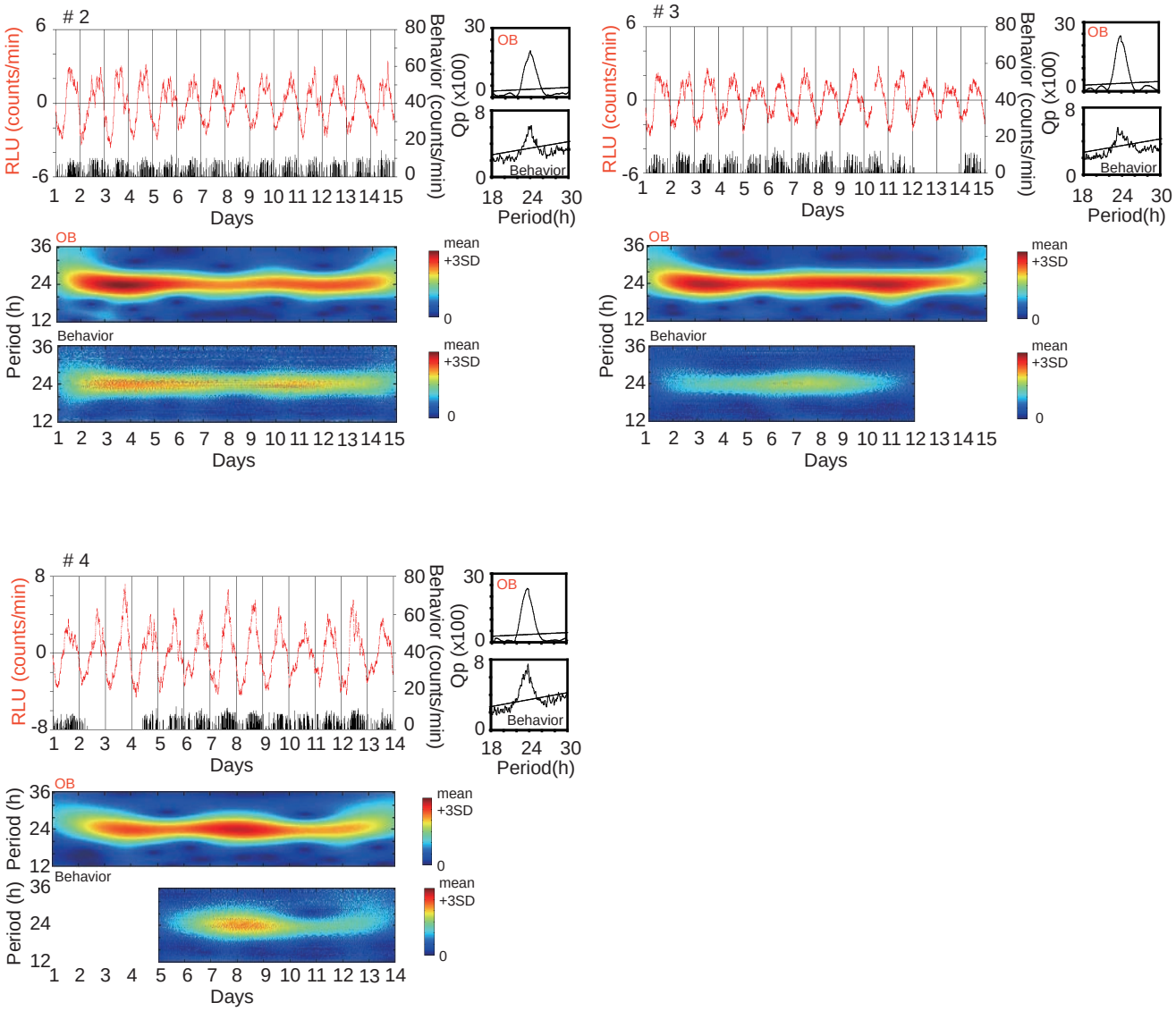

Figure S1

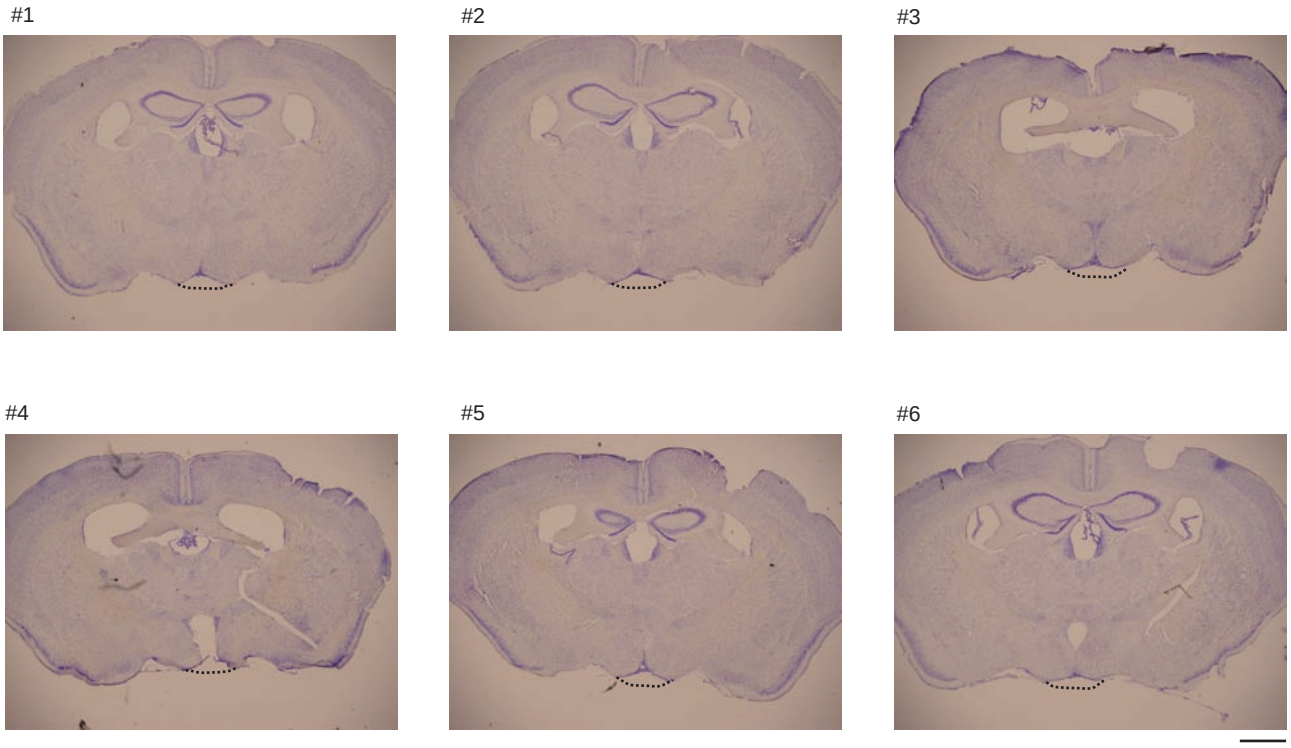

Figure S2

SCN lesion

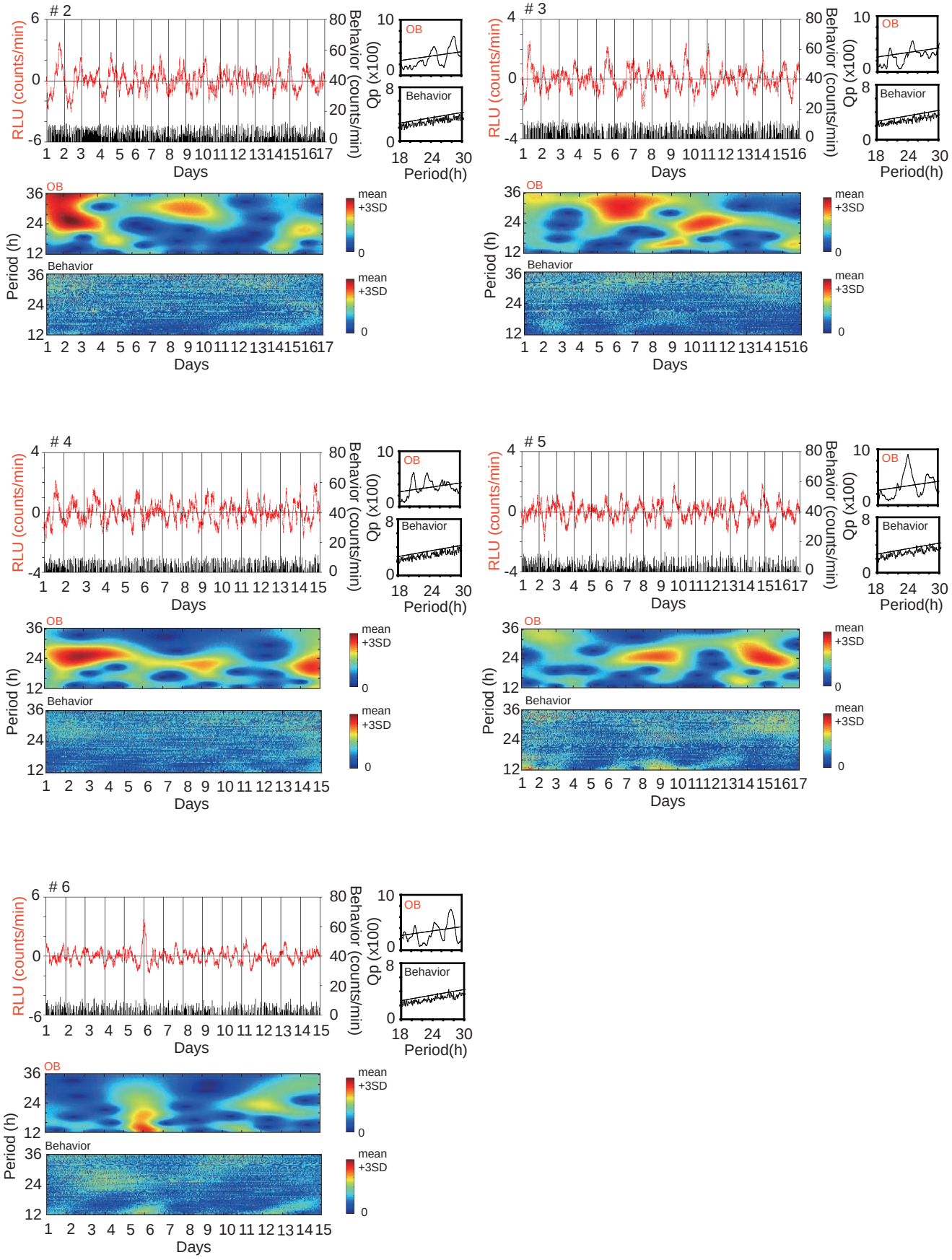

Figure S3

Vipr2$^{-/-}$

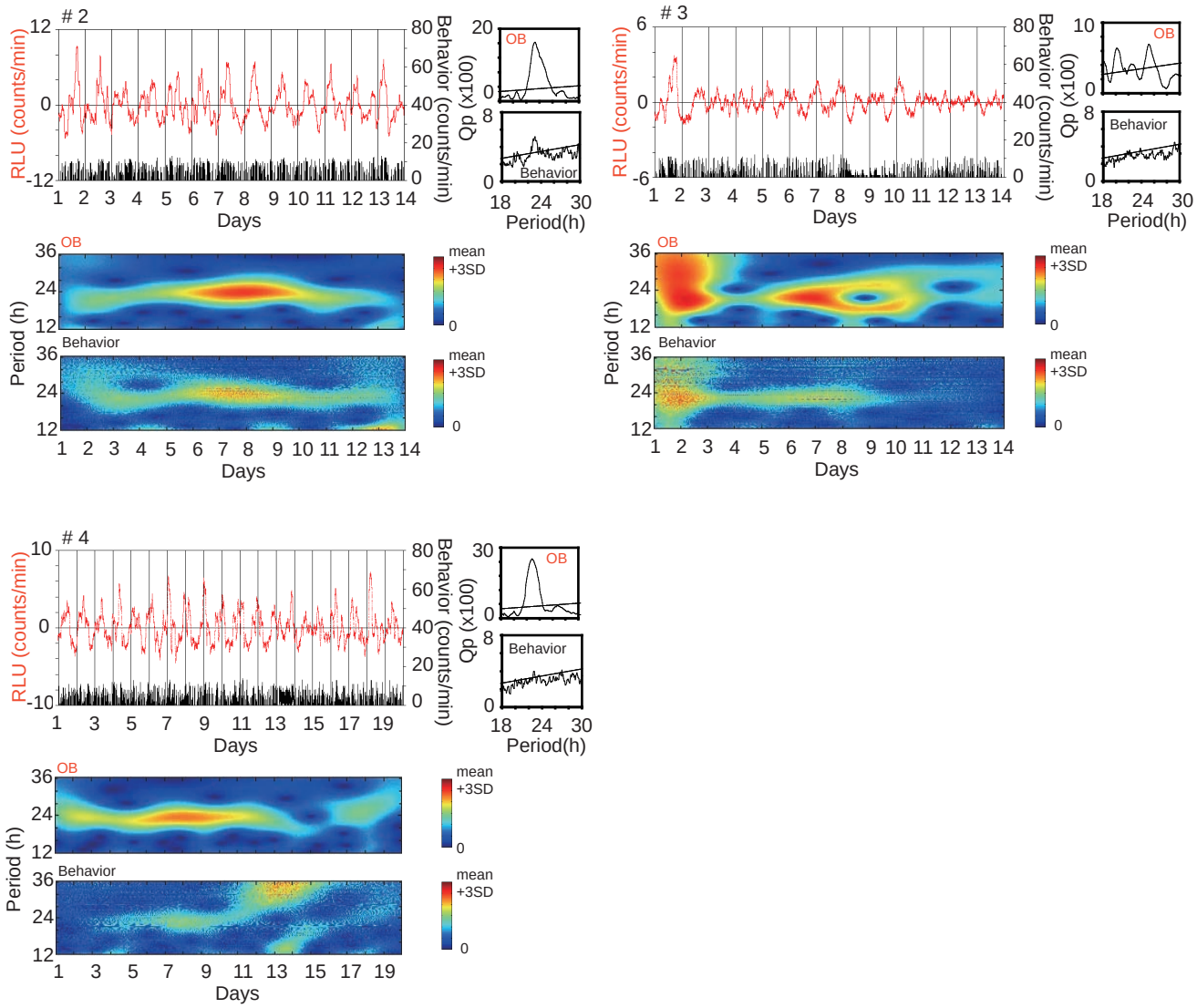

Figure S4